BUTTERWORTH HEINEMANN

Polymer Vol. 36 No. 19, pp. 3711–3717, 1995

0032-3861/95/$10.00+0.00

Phase behaviour of polymer/solvent/non-solvent systems

Young Soo Soh*
Department of Chemical Engineering, Taegu University, Jinryang-myun, Kyungsan-gun, Kyungbook, Korea

and Jeong Ho Kim
Department of Chemical Engineering, Suwon University, Suwon, Kyungkee-do, Korea

and Carl C. Gryte
Department of Chemical Engineering, Columbia University, New York, NY, USA
(Received 18 July 1994; revised 7 February 1995)

For three-component systems composed of a crystalline polymer (component 3), solvent (component 2) and non-solvent (component 1), polymer-poor liquid–polymer-rich liquid and liquid–polymer crystal phase equilibrium lines are constructed. When the two lines overlap, four regions of different phase separations are distinguished. For these systems, the Gibbs free energy change of mixing surface is constructed and the equilibrium line is then a collection of points where a common tangent plane touches the Gibbs free energy change of mixing surface. Based on the Flory–Huggins theory, computer programs are developed for phase diagram construction and the Gibbs free energy change of mixing surface, and the diagrams and Gibbs free energy change of mixing surface for the poly(vinylidene fluoride)/dimethylformamide/octanol system are presented.

(Keywords: phase diagram; binodal line; spinodal line)

INTRODUCTION

In three-component systems composed of a crystalline polymer (component 3), solvent (component 2) and non-solvent (component 1), two types of phase separation phenomena can be distinguished. These are (1) polymer-poor liquid–polymer-rich liquid phase separation and (2) liquid–polymer crystal phase separation. Liquid–liquid phase separation occurs in an attempt to lower the overall Gibbs free energy according to the second law of thermodynamics. This phase equilibrium is significant in many polymer solution processes including membrane casting and other polymer solution coagulation processes[1,2]. For ternary systems involving stereo-regular polymers such as poly(vinylidene fluoride) (PVdF), in addition to equilibrium between a polymer-poor liquid phase and a polymer-rich liquid phase there is the possibility of equilibrium between a liquid phase and a crystalline solid polymer phase in the region of high polymer content when the temperature is lowered[3,4]. The presence of crystallinity may result in a gel structure or in the formation of discrete polymer particles (a globular non-cohesive structure).

In this work, based on the Flory–Huggins theory, computer programs are developed for phase diagram construction and the diagrams for the poly(vinylidene fluoride) (PVdF)/dimethylformamide (DMF)/octanol system are presented. In addition, the Gibbs free energy change of mixing surface for the system is drawn to complement the understanding of the phase diagrams.

* To whom correspondence should be addressed

THEORY

Liquid–liquid phase equilibrium

Binodal line. The conditions or equilibrium criteria which must be satisfied in order for equilibrium to exist between two liquid phases in a three-component system can be rewritten as

$$\mu_i = \mu_i' \qquad i = 1,2,3 \tag{1}$$

where the prime ($'$) denotes the second phase. The chemical potentials μ_1, μ_2 and μ_3 of the non-solvent, solvent and polymer, respectively, for a ternary system are well known to be represented by functions of the ϕ_i; V_1, V_2 and V_3, the molar volumes of the respective species; χ_{ij}, the pair interaction parameters, which are dimensionless quantities that characterize the interaction energy per molecule i divided by kT; and temperature T[5–7]. To obtain the equilibrium points, these expressions are substituted into equation (1), and for a given ϕ_1, volume fraction of component 1, three unknowns are computed. The Newton–Raphson method is employed to solve these simultaneous equations with three unknowns.

Spinodal line. The spinodal line separates the two-phase region into unstable and metastable regions. For two-component systems, a composition region is unstable if $d^2G/d\phi_1^2 < 0$, and metastable if $d^2G/d\phi_1^2 > 0$. The boundary, where $d^2G/d\phi_1^2 = 0$, is called the spinodal point. For three-component systems, the spinodal point, a collection of which becomes the spinodal line, is obtained on a plot of Gibbs free energy *versus* composition along the tie line (for example, line B in *Figure 4*). On this plot, a composition is unstable if $d^2G/d\phi_1^2 < 0$, a composition is metastable if $d^2G/d\phi_1^2 > 0$, and $d^2G/d\phi_1^2 = 0$ represents a spinodal point. A spinodal point is obtained for each tie line, and a collection of these points becomes the spinodal line. To obtain an expression for $d^2G/d\phi_1^2$ as a function of only one independent variable, for example ϕ_1, G should be recast as a function of ϕ_1. Firstly, the Flory–Huggins expressions for the chemical potentials μ_1, μ_2 and μ_3 in terms of ϕ_i are substituted into

$$G = n_1\mu_1 + n_2\mu_2 + n_3\mu_3$$

or

$$G = \frac{\phi_1}{V_1}\mu_1 + \frac{\phi_2}{V_2}\mu_2 + \frac{\phi_3}{V_3}\mu_3 \tag{2}$$

where V_i is the molar volume of component i. This recasts the equation as a function of ϕ_1, ϕ_2 and ϕ_3. The sum of the volume fractions is always unity, so the equation can be written in terms of two independent variables. In this work, ϕ_3 is substituted by $1 - (\phi_1 + \phi_2)$, and the independent variables for the equation are then ϕ_1 and ϕ_2. Also, the tie lines which were obtained in the computation process for the liquid–liquid equilibrium (binodal) lines can be represented by

$$\phi_2 = a\phi_1 + b \tag{3}$$

In equation (3), a and b are constant for each tie line. Substituting equation (3) into the above-mentioned G formula that has ϕ_1 and ϕ_2 as independent variables, G becomes a formula that has only one independent variable, ϕ_1.

These equations for G, $dG/d\phi_1$ and $d^2G/d\phi_1^2$ can be found elsewhere[2].

Liquid–solid phase equilibrium

At high polymer concentration and low temperature, the Gibbs free energy of the solution is lowered by the formation of a crystalline polymer. At equilibrium, the polymer crystal is in contact with a liquid which contains some polymer. Since the polymer crystal is pure, the chemical potential of the crystalline polymer repeat unit is given by[2]

$$\mu_u^c - \mu_u^\circ = -\Delta H_u(1 - T/T_M^\circ) \tag{4}$$

The chemical potential of the polymer repeat unit in a polymer solution may be written as

$$(\mu_u - \mu_u^\circ)/RT = (V_u/V_3)[\ln\phi_3 + (1 - \phi_3) \times (1 + \chi_{13}\phi_1 V_3/V_1 + \chi_{23}\phi_2 V_3/V_2) - \phi_1(1 + \chi_{12}\phi_2)V_3/V_1 - \phi_2 V_3/V_2] \tag{5}$$

By substituting equations (4) and (5) into

$$\mu_u = \mu_u^c \tag{6}$$

we get

$$-\Delta H_u/R(1/T - 1/T_M^\circ) = (V_u/V_3)[\ln\phi_3 + (1 - \phi_3) \times (1 + \chi_{13}\phi_1 V_3/V_1 + \chi_{23}\phi_2 V_3/V_2) - \phi_1(1 + \chi_{12}\phi_2)V_3/V_1 - \phi_2 V_3/V_2] \tag{7}$$

For a given ϕ_1, ϕ_2 can be solved in this equation, thus defining the equilibrium line. The Newton–Raphson method is again employed to solve the equation.

The Gibbs free energy change of mixing

By definition, the Gibbs free energy change of mixing (ΔG_M) is given by

$$\Delta G_M = G - \Sigma x_i G_i^\circ \tag{8}$$

where G_i° is the molar Gibbs free energy of i in a specified standard state (the pure state at the same temperature and pressure as the solution) and G is the molar Gibbs free energy of the solution. The equation

$$G = \Sigma x_i \bar{G}_i \tag{9}$$

relates the molar Gibbs free energy of the solution to the partial Gibbs free energy $\bar{G}_i$. Substitution of this expression for G into equation (8) gives

$$\Delta G_M = \Sigma x_i \bar{G}_i - \Sigma x_i G_i^\circ \tag{10}$$

Since $\bar{G}_i = \mu_i$ and $G_i^\circ = \mu_i^\circ$, equation (10) may be written as

$$\Delta G_M = \Sigma x_i(\mu_i - \mu_i^\circ) \tag{11}$$

ΔG_M is the difference between the Gibbs free energy of the solution and the sum of the properties of the pure components that make up the solution.

The Gibbs free energy change of mixing per unit volume ($\Delta G_M/V_M$) is given by

$$\Delta G_M/V_M = \Sigma(\phi_i/V_i)(\mu_i - \mu_i^\circ) \tag{12}$$

RESULTS AND DISCUSSION

The computer programs were written in Fortran and are detailed elsewhere[2]. The binary interaction parameters were obtained according to a method given elsewhere[2]. The physical properties used in the computations are shown in *Table 1*.

Figure 1 shows the phase diagram for the PVdF/DMF/octanol system. For temperatures of 300, 340, 380, 420 and 460K, binodal lines, spinodal lines and crystallization lines are shown in the same diagram. Phase diagrams for temperatures other than these may be computed but a minimal number of temperatures are shown here for the sake of clarity. On this figure, the ternary critical points are not clear. However, there are some critical points off the DMF–octanol axis which are

Table 1 Physical properties of the components

Component	Molecular weight M_w	Density (g cm^{-3})	Melting point (°C)
PVdF	2.16×10^6	1.75–1.78[a] 1.675–1.681[b]	
DMF	73.10	0.9445	−61
Octanol	130.23	0.827	−15

[a] Crystalline
[b] Amorphous

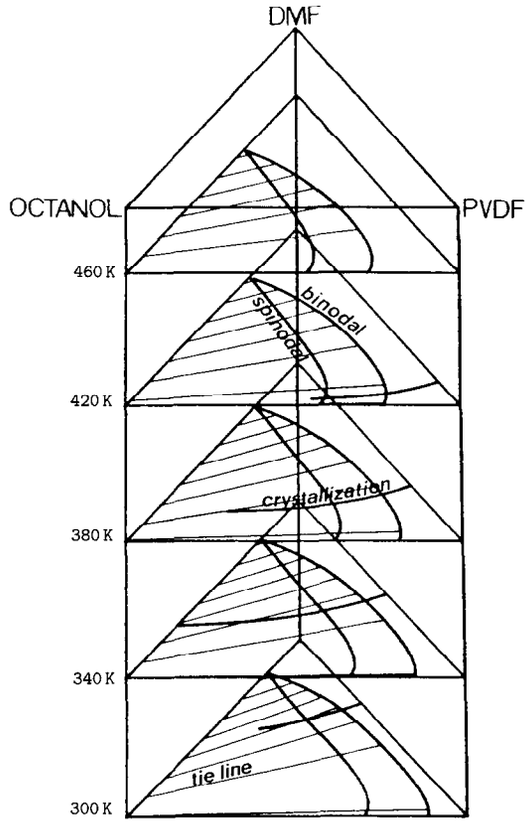

Figure 1 Phase diagram for the PVdF/DMF/octanol system. At high temperature (460 K) above the melting point of PVdF, only liquid–liquid phase separation occurs. For the other temperatures, the liquid–crystal phase separation equilibrium line overlaps the liquid–liquid phase separation equilibrium line. The thinner lines represent tie lines for the liquid–liquid phase separation

visible with a higher magnification of the figure. It has been shown that as the molecular weight of the polymer increases, the ternary critical point moves closer to the solvent–non-solvent axis[2]. It has also been shown that as the molecular weight of the polymer increases, a smaller quantity of polymer exists in the polymer-poor phase. Consequently, for a very high molecular weight polymer, most of the tie lines end very close to or at the DMF–octanol axis. In our computations, we set the volume fraction of the polymer in the polymer-poor liquid phase as an unknown, and we also set the volume fraction of polymer to zero, resulting in the same or very similar results. In *Figure 1*, the binodal surface, spinodal surface and crystallization surface can be pictured as imaginary. Some tie lines for the liquid–liquid phase equilibrium are drawn in the figure but tie lines for the liquid–solid phase equilibrium are not. The tie lines for the liquid–solid phase equilibrium are those which connect the 100% PVdF point to any point on the liquid–solid phase equilibrium line, but these are not drawn in *Figure 1*. The effect of temperature on the phase diagram is very clearly shown in this figure. As the temperature is lowered, the two-phase region with respect to liquid–liquid phase equilibrium becomes large, and the two-phase region with respect to liquid–solid phase equilibrium also becomes large.

The effect of temperature is more significant for the liquid–solid phase equilibrium line. For example, at temperatures higher than the melting temperature of pure PVdF, no phase separation with respect to liquid–solid phase equilibrium will be observed. However, the liquid–liquid phase equilibrium line still exists at this temperature.

Using equation (12), the dependence of the Gibbs free energy change of mixing per unit volume on composition for the PVdF/DMF/octanol system can be depicted as shown in *Figure 2*.

The phase equilibrium criterion represented by equation (1) is mathematical. If we consider phase separation on the Gibbs free energy change of mixing curve for a binary system, the binodal points or equilibrium points are points where a common tangent coming from the bottom of the plot touches the free energy curve. At compositions inside these points, the Gibbs free energy becomes lowered by separation of the system into two phases. Likewise, in three-component systems, binodal points or equilibrium points are points where a common tangent plane (which comes from the bottom of *Figure 2*) touches the Gibbs free energy change of mixing surface. The total Gibbs free energy is a minimum for two phases that have compositions represented by two points connected by the common tangent plane for any overall composition represented by a point on the line connecting these two points. The surface of *Figure 2* has two ridges (ridges if viewed from the bottom of the paper, valleys if viewed from the top of the page). (In this work, as we probe the surfaces to locate the common tangent points, we will use the word 'ridge' not the word 'valley', even though we see valleys in the figures.) A plane in *Figure 2* would create collections of common tangent points by rolling of that plane. This collection of points would be a binodal line. Careful observation of *Figure 2* shows a very sharp ridge along or very near the DMF–octanol line and another ridge which is polymer rich. A very sharp ridge along or near the DMF–octanol line is characteristic of this system with high molecular weight polymers. For the purpose of presentation, the same surface was turned around 180°.

Location of the ridges is made easier by comparing the surface in *Figure 2* with the computation results of *Figure 1*. The observed ridge of the polymer-rich phase is drawn in *Figure 3*. The location of ridges verifies the accuracy or validity of the computed binodal line. Visual location of the spinodal lines in *Figure 2*, however, is a little more difficult.

To complement the free energy surface, the curves for the free energy change of mixing are shown in *Figure 4*. All the lines except B and I are arbitrary. B and I are real tie lines. A common tangent to B and I can be used to locate the equilibrium point.

To examine the effects of B_{13} on the configuration of the free energy surface for the PVdF/DMF/octanol system[2,8], two different values were used and the results were compared elsewhere[2]. It was found that the overall effect of B_{13} are not very significant. The interaction parameters used are summarized in *Table 2*.

In *Figure 5*, the phase diagram for 300 K is drawn. At this temperature both crystallization and liquid–liquid phase separation are thermodynamically possible. Consider a composition represented by X. Assuming the crystallization process is kinetically the slower[3], liquid–liquid phase separation will occur first[9] to give two phases, represented by E (polymer-rich liquid phase) and

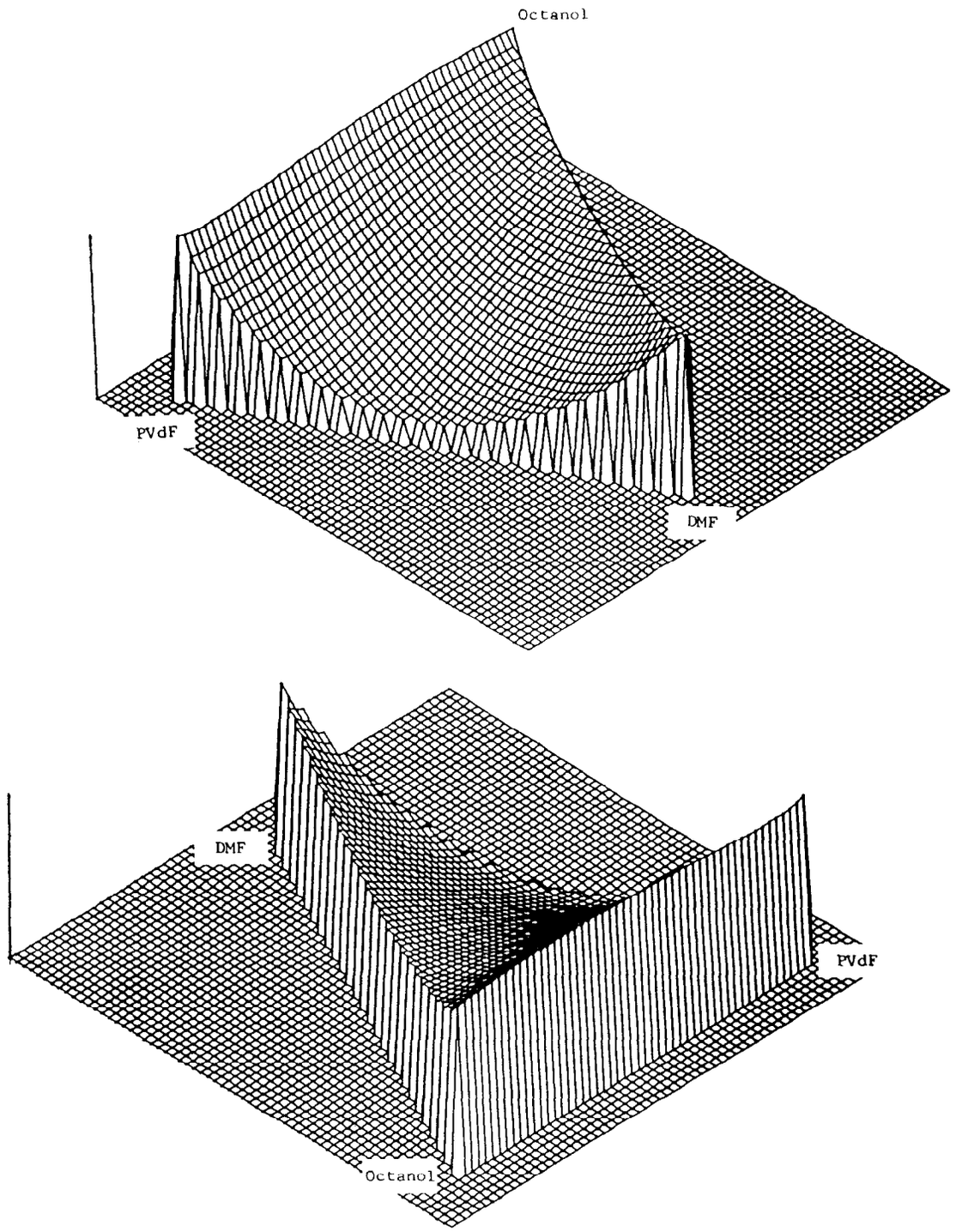

Figure 2 The Gibbs free energy change of mixing per unit volume for the PVdF/DMF/octanol system. The values of B_{12}, B_{13} and B_{23} are given in *Table 2*. The bottom surface represents an energy of $-8.94\,\text{cal}\,\text{cm}^{-3}$. $\Delta G_M/V_M = 0$ for the pure components

F (polymer-poor liquid phase). However, the phase represented by E is unstable with respect to the liquid–solid phase equilibrium. Thus, E will again separate into two phases – a pure crystal phase P and a second liquid phase G. At this point, before the liquid phase reaches the concentration represented by G, this phase (represented by an arbitrary point along the line EG) will become unstable with respect to the liquid–liquid phase diagram. Eventually, solution X and any solution represented by the composition inside triangle IRP (IR being a tie line) will separate into three phases represented by compositions I, R and P. Thus, as shown in *Figure 5*, we have four regions in the isothermal phase diagram, each showing a different phase separation behaviour:

1. region IHR represents a polymer-poor liquid (IH)–polymer-rich liquid (HR) phase separation;
2. region KRP represents a polymer crystal (P)–liquid (RK) phase separation;

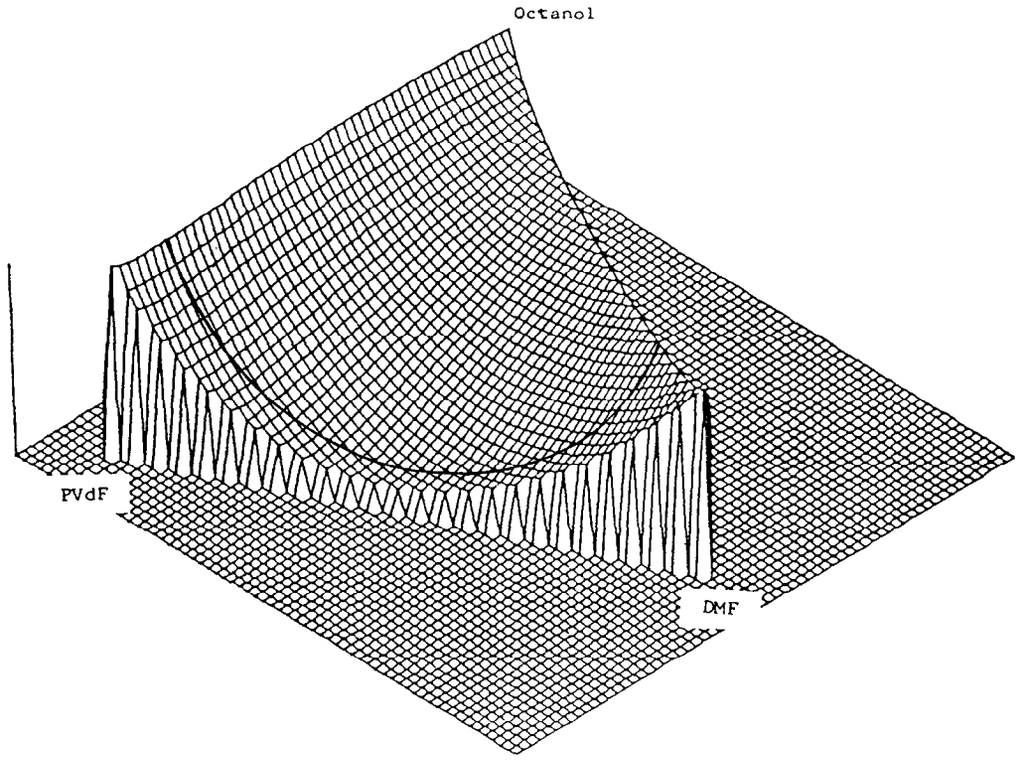

Figure 3 Location of the polymer-rich phase equilibrium line for *Figure 2*

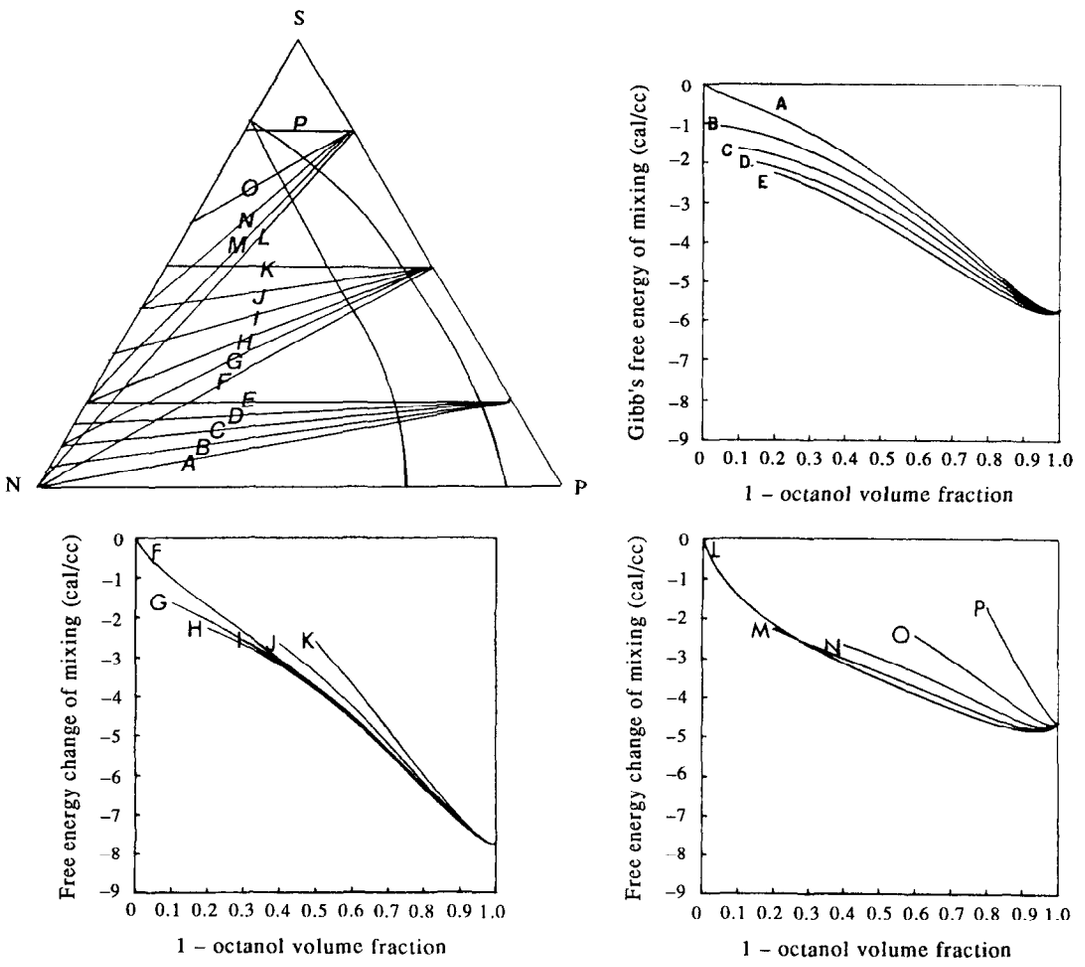

Figure 4 Gibbs free energy changes of mixing curves. Lines B and I are tie lines, others are arbitrary lines

Table 2 Interaction parameters for the PVdF/DMF/octanol system

B_{12}	5.534 cal cm^{-3}
B_{13}	6.248 cal cm^{-3}
B_{23}	−20.299 cal cm^{-3}

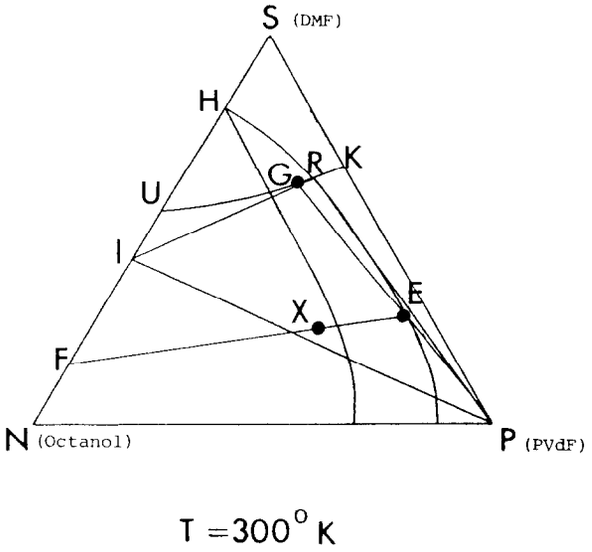

Figure 5 Theoretical consideration of the phase diagram. Point G is on curved equilibrium line UR. Lines IR and FE are tie lines. Line RK is a curved equilibrium line, continued from line UR

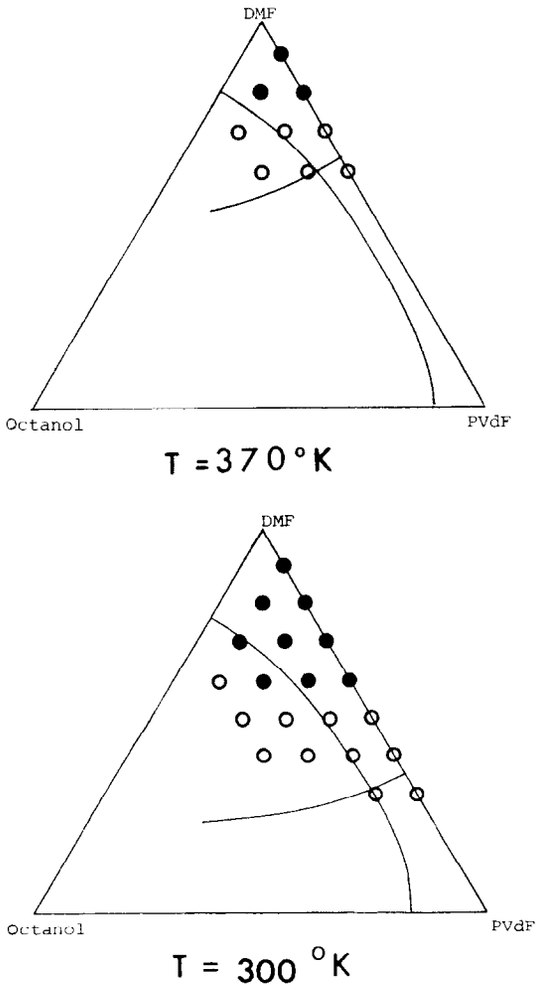

Figure 6 Phase equilibrium lines for an experimental mixture: (●) homogeneous; (○) heterogeneous

3. region IRP represents a phase separation with three phases, namely polymer-poor liquid (I), polymeric crystal (P) and polymer-rich liquid (R); and
4. region INP represents a polymer-poor liquid (IN)–polymer crystal (P) phase separation.

EXPERIMENTAL

Cloudiness was observed for well-mixed polymer solutions. Appropriate amounts of PVdF, DMF and octanol were weighed in small glass tubes which were degassed, flushed with nitrogen, degassed again and sealed under vacuum. The mixtures in the sealed glass tubes were then heated in a hot air oven at approximately 200°C for at least 24 h in order to obtain a homogeneous liquid mixture. Then, the samples were cooled to the desired temperature and kept there for another 24 h. After this period, the tubes were inspected visually and with polarized light to check for phase separation. Some of the results are shown in *Figure 6*. Although qualitative in nature, these data are consistent with the computed phase equilibrium lines. At both temperatures, some of the points in the theoretically single-phase region show cloudiness experimentally. For example, at 370 K, a 70/30 DMF/PVdF composition should be one homogeneous phase, but the experiment shows phase separation. This, we believe, happened because a small quantity of DMF evaporated during the degassing step while preparing the samples. A similar explanation applies to the open circles (*Figure 6*) in the homogeneous phases.

In this experiment, the homogeneous region was differentiated from the heterogeneous region but the differences between liquid–liquid phase separation (region IHR), and liquid–crystal phase separation (region KRP) were not confirmed. We tried and will try in the future to differentiate the two different phase separations by taking advantage of the fact that liquid–crystal phase separations can be detected with polarized light, whereas liquid–liquid phase separations cannot. With liquid–liquid phase separation, turbidity would be observed visually and polarized light would not change the picture very much. With liquid–crystal phase separation, turbidity would also be observed visually and polarized light would reveal the presence of spherulites. As the liquid–liquid phase separation is relatively fast and crystallization is believed to be slower, the measurements could be made as a function of time: rapid development of turbidity would come from liquid–liquid phase separation, whereas a slower development of turbidity would come from liquid–crystal phase separation.

As the differences between liquid–liquid phase separation and liquid–crystal phase separation were not discernible for the three-phase region IRP, which always showed cloudiness in the experiments, differentiation between the polymer crystal and polymer-rich phases was not possible at this point and neither was confirmation of the phase separation into three phases. Even with the above-mentioned knowledge, it will be difficult to differentiate the polymer crystal phase from the polymer-rich liquid phase because the opaqueness of the polymer crystal hides the turbidity due to the liquid–liquid phase separation. However, if the measurements were performed as a function of time, liquid–liquid

phase separation would first give some turbidity, then crystallization would hide the turbidity due to the liquid–liquid phase separation.

CONCLUSIONS

For three-component systems composed of a crystalline polymer (component 3), solvent (component 2) and non-solvent (component 1), polymer-poor liquid–polymer-rich liquid phase equilibrium lines and liquid–polymer crystal phase equilibrium lines can be constructed. For the polymer-poor liquid–polymer-rich liquid phase equilibrium, spinodal lines can also be drawn. The two lines overlap over a wide temperature range, and four regions of different phase separations can be distinguished.

REFERENCES

1 Cohen, C., Tanny, G. B. and Prager, S. *J. Polym. Sci., Polym. Phys. Edn* 1979, **17**, 477
2 Soh, Y. S. PhD Dissertation, Columbia University, New York, 1986
3 Broens, L., Altena, F. W., Smolders, C. A. and Koenhen, D. M. *Desalination* 1980, **32**, 33
4 Bokhorst, H., Altena, F. W. and Smolders, C. A. *Desalination* 1981, **38**, 349
5 Tompa, H. *Trans. Faraday Soc.* 1949, **45**, 1142
6 Tompa, H. 'Polymer Solutions', Butterworths, London, 1956, Ch. 7
7 Koningsveld, R. 'Polymer Science' (Ed. A. D. Jenkins), Elsevier, New York, 1972
8 Brandrup, J. and Immergut, E. H. 'Polymer Handbook', Wiley, New York, 1966
9 Booth, C. and Price, C. *Polymer* 1966, **7**, 85